

# Transient-signal-based sample-detection in atomic force microscopy

Deepak R. Sahoo, Abu Sebastian, and Murti V. Salapaka<sup>a)</sup>

Department of Electrical and Computer Engineering, Iowa State University, Ames, Iowa 50011

(Received 11 July 2003; accepted 12 September 2003)

In typical dynamic mode operation of atomic force microscopes, steady state signals like amplitude and phase are used for detection and imaging of material. In these methods, the resolution and bandwidth are dictated by the quality factor ( $Q$ ) of the cantilever. In this letter, we present a methodology that exploits the deflection signal during the transient of the cantilever motion. The principle overcomes the fundamental limitations on the trade off between resolution and bandwidth present in existing methods and makes it independent of the quality factor. Experimental results provided corroborate the theoretical development. © 2003 American Institute of Physics.

[DOI: 10.1063/1.1633963]

Atomic force microscopes<sup>1</sup> (AFMs) utilize a cantilever to image and manipulate sample properties at the atomic scale. The dynamic mode of operation (where the cantilever is oscillated near its first resonance frequency and the changes in the cantilever oscillations are monitored to infer sample properties) is an attractive mode of imaging primarily due to its gentle nature on the sample.<sup>2</sup> In this mode of operation, cantilevers with high quality factors are employed essentially for high resolution. However, due to high quality factor, the settling time is large, that constrains the steady state signal (like the demodulated amplitude and phase) based methods to have a small bandwidth. Using active  $Q$  control the bandwidth or the resolution can be increased;<sup>3-5</sup> however, the trade off between bandwidth and resolution remains inherent.<sup>4</sup> The existing methods do not utilize the cantilever model and do not exploit the deflection signal during the transient state of the cantilever.

In this letter we present a principle that harnesses the transient part of the cantilever dynamics. As in steady state methods, high quality factors result in high resolution; however, in the method presented, the bandwidth is largely independent of the quality factor  $Q$  and is determined by the resonant frequency of the cantilever. As is seen later it also provides advantages with respect to resolution; particularly of events that have very small time scales.

When the cantilever is forced sinusoidally at its first resonance frequency, its dynamic response is well described by the first mode model given by

$$\begin{aligned} \dot{x} &= \underbrace{\begin{bmatrix} 0 & 1 \\ -\omega_0^2 & -\frac{\omega_0}{Q} \end{bmatrix}}_A x + \underbrace{\begin{bmatrix} 0 \\ 1 \end{bmatrix}}_B (\eta + w), \\ y &= \underbrace{\begin{bmatrix} 1 & 0 \end{bmatrix}}_C x + v, \end{aligned} \tag{1}$$

where  $x = [p \ v]^T$ ,  $Q$ ,  $\omega_0$ ,  $\eta$ ,  $w$ ,  $y$ , and  $v$  denote the

cantilever-tip position ( $p$ ) and velocity ( $v = \dot{p}$ ), the quality factor, the first resonant frequency, the thermal-noise, external forces acting on the cantilever, the deflection signal, and the measurement (photodiode) noise, respectively. The cantilever model described earlier can be identified precisely using the thermal-noise response.<sup>6</sup> The cantilever can be imagined to be a system that takes in the thermal-noise  $\eta$ , the dither signal  $g$ , the tip-sample interaction force  $\phi(x)$  as inputs (in which case  $w = \phi + g$ ), and produces the photodiode signal  $y$  as the output.

The transient signal based detection method relies on the construction of an observer (see Fig. 1) that provides an estimate of the state  $x$  of the cantilever. The observer dynamics is given by

$$\dot{\hat{x}} = A\hat{x} + Bg + L(y - \hat{y}); \quad \hat{x}(0) = \hat{x}_0, \quad \hat{y} = C\hat{x}, \tag{2}$$

and associated state estimation error ( $\tilde{x} := x - \hat{x}$ ) dynamics is given by

$$\dot{\tilde{x}} = (A - LC)\tilde{x} + B\eta - Lv; \quad \tilde{x}(0) = x(0) - \hat{x}(0). \tag{3}$$

The observer mimics the dynamics of the cantilever [given in Eq. (1)]. It utilizes a correcting term  $L\tilde{y}$  where  $L$  is the gain of the observer and  $\tilde{y} = y - \hat{y} = C\tilde{x} = e$  is the error in estimating the deflection signal. The error  $\tilde{x}$  between the estimated state  $\hat{x}$  and the actual state  $x$  of the cantilever, when no noise terms are present ( $\eta = v = 0$ ) is only due to the mismatch in the initial state of the observer and the cantile-

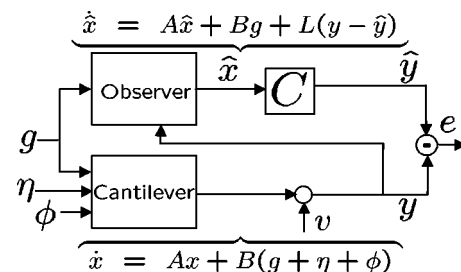


FIG. 1. The observer estimates the state to be  $\hat{x}$  in presence of thermal noise  $\eta$  and measurement noise  $v$ . The actual state is  $x$ . By a choice of the observer gain  $L$  the error  $e$  in the state estimate goes to zero when the cantilever is freely oscillating. When the cantilever is subjected to the sample force  $\phi$ , its dynamics is altered whereas the observer dynamics remains the same. This is registered as a nonzero value in the error  $e$ .

<sup>a)</sup>Electronic mail: murti@iastate.edu

ver [see Eq. (3)]. The error  $\bar{x}$  goes to zero when the real part of all the eigenvalues of the matrix  $(A-LC)$  are negative. Since the pair  $(A, C)$  is *observable* for the cantilever model (i.e.,  $\text{rank}([A \ C]^T) = 2$  when a second order model is assumed) the eigenvalues of the matrix  $A-LC$  can be placed anywhere by appropriately choosing  $L$ .<sup>7</sup> Thus, the error signal  $e$  due to initial condition mismatch can be reduced to zero and in principle arbitrarily fast by suitably choosing  $L$ . When there is a change in the tip-sample interaction the cantilever dynamics is effected. This introduces an error in tracking which evolves according to the cantilever-observer dynamics as given by Eq. (3). Also, when the change in the tip-sample potential persists, the observer by utilizing its input  $y$  may track the altered cantilever state. It can also be shown that in the presence of noise sources  $\eta$  and  $v$  the error signal  $e$  is a zero-mean stationary process. Thus, the error signal shows the signature of the change in the tip-sample behavior (buried in noise) immediately after the change is introduced. The error  $e$  may recover its zero mean nature even when the interaction change persists. This is in contrast to the steady state methods where the information is available not in the initial part but after the cantilever has come to a steady state. The Kalman observer<sup>8</sup> can be employed for optimal tracking in which case the error process (also known as the *innovation*) has zero mean and is white during perfect tracking.

The error profile due to a tip-sample interaction change can be better characterized if a model of the effect of the tip-sample interaction change on the cantilever-motion is available. We assume that the sample's influence on the cantilever tip is approximated by an impact condition where the tip-position and velocity instantaneously assume a new value (equivalent to resetting to a different initial condition). This is satisfied in most typical operations because in the dynamic mode, the time spent by the tip under the sample's influence is negligible compared to the time it spends outside the sample's influence.<sup>9</sup> The assumption is also corroborated by experimental results provided later.

The error dynamics [characterized in the Laplace domain from Eq. (3)] is given by

$$e(s) = \frac{\eta(s) + \left(s^2 + \frac{\omega_0}{Q}s + \omega_0^2\right)v(s) + \left(s + \frac{\omega_0}{Q}\right)v_1 + v_2}{s^2 + \left(\frac{\omega_0}{Q} + l_1\right)s + \left(\omega_0^2 + l_2 + \frac{\omega_0}{Q}l_1\right)}, \quad (4)$$

where  $(v_1, v_2)^T$  is the initial condition reset due to change in tip-sample interaction and  $L = (l_1 \ l_2)^T$  is the gain of the observer that must satisfy the stability criterion:  $[(\omega_0/Q) + l_1] > 0$  and  $[\omega_0^2 + (\omega_0/Q)l_1 + l_2] > 0$ .

From Eq. (4) it can be seen that the tracking bandwidth is characterized by

$$B \propto \frac{\omega_0}{Q} + l_1. \quad (5)$$

Since the choice of the gain term  $l_1$  is independent of the quality factor  $Q$ , the tracking bandwidth of the observer is effectively decoupled from  $Q$ .

From Eq. (4), it can be shown that with increasing values of  $l_1$  and  $l_2$ , the bandwidth  $B$  and the signal to noise ratio

$\text{SNR}_{\text{th}}$  (in the error signal  $e$ ) due to thermal noise increase and the signal to noise ratio  $\text{SNR}_v$  due to photodiode noise decreases. Therefore, the bandwidth constraint in the detection scheme is mainly imposed by the measurement noise. It is evident that a desired trade off between signal to noise ratio and bandwidth can be obtained by an appropriate choice of  $l_1$  and  $l_2$  that is independent of  $Q$ . This provides considerable flexibility when compared to existing steady state methods where  $Q$  determines the bandwidth. For typical cantilever parameters and ambient conditions, the Kalman design yields a bandwidth  $B \gg \omega_0/Q$  and the innovation process carrying the signature of tip-sample interaction has a zero mean and white component. Note that the observer gain  $l_1$  can be chosen large enough so that the cantilever state is tracked within a couple of cycles of the dither forcing. This shows that the optimal bandwidth is primarily dictated by the resonant frequency  $\omega_0$  of the cantilever.

The sample detection problem is formulated by considering a discretized model of the cantilever [given in Eq. (1)] and the impact model for the tip-sample interaction, as described by

$$\begin{aligned} x(i+1) &= Fx(i) + Gg(i) + G_1\eta(i) + \delta_{\theta, i+1}\nu, \\ y(i) &= Hx(i) + v(i); i \geq 0, \end{aligned} \quad (6)$$

where  $\delta_{i,j}$  denotes the dirac delta function,  $\theta$  denotes the time instant when the tip-sample impact occurs and  $\nu$  signifies the magnitude of the impact. It is assumed that the thermal noise and the photodiode noise are white and uncorrelated. As indicated before, given this statistics, the optimal observer is a Kalman observer.<sup>8</sup> With an observer having gain  $K$  (the discrete-time equivalent of  $L$ ), the innovation sequence  $e(i)$  is given by<sup>10</sup>

$$e(i) = Y(i; \theta)\nu + e^w(i), \quad (7)$$

where  $Y(i; \theta) = [H; H(F-KH); \dots H(F-KH)^{i-\theta}]$  and  $e^w(i)$  is the innovation sequence when  $\nu=0$ .  $Y(i; \theta)$  is a dynamic profile with unknown arrival time  $\theta$ . When there is no change in tip-sample interaction (i.e.,  $\nu=0$ ) the innovation sequence has zero mean and is white.<sup>10</sup> When there is a change in tip-sample interaction the innovation sequence becomes nonwhite and is sum of a zero mean and white sequence  $e^w(i)$  and  $Y(i; \theta)\nu$  with  $\theta$  and  $\nu$  unknown.

Thus, the objective of detecting a change in tip-sample interaction is translated to the task of detecting the dynamic profile  $Y(i; \theta)\nu$  in a zero mean white sequence. This problem can be cast in hypothesis testing framework as

$$\begin{aligned} H_0: Y_i &= e^w(i), \quad i = 1, 2, \dots, n, \\ H_1: Y_i &= Y(i; \theta)\nu + e^w(i), \quad i = 1, 2, \dots, n, \end{aligned} \quad (8)$$

where the observed data  $Y_i = e(i)$  is the innovation sequence. The dynamic profile is detected by using a likelihood ratio test<sup>10,11</sup> and a decision signal is obtained.

The advantages of the methodology are well demonstrated in the following experiment performed using a Digital Instruments multimode AFM. A cantilever with first resonance frequency  $f_0 = 70.1$  kHz and quality factor  $Q = 180$  was forced at  $f_0$  to an amplitude of 80 nm. A 0.5 V pulse

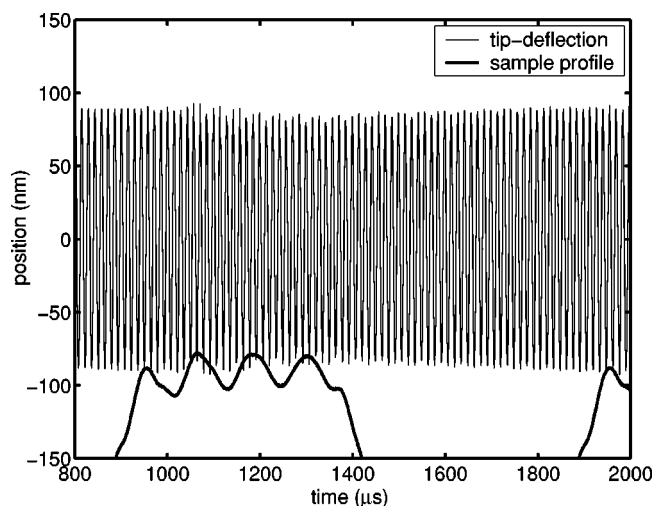


FIG. 2. Cantilever-tip deflection data with respect to approximate sample position is shown. Note that from the amplitude profile of the deflection signal the four peaks in the sample profile are not discernible.

train having 1 ms time period and duty cycle of 50% was applied to the piezoscanner holding an highly oriented pyrolytic graphite sample. Each pulse applied to the piezo generated a sample profile (see Fig. 2) having four peaks separated by approximately 100  $\mu\text{s}$ . The sample was brought close to the cantilever so that the tip would interact with the four peaks in the sample profile. Since the settling time of the cantilever is in the order of  $Q/f_0 \approx 2.57$  ms, the cantilever was interacting with the peaks in the sample profile during its transient state and it never recovered the steady state during the experiment. From the amplitude profile of the deflection signal (see Fig. 2), it is not possible to detect the four peaks in the sample profile. Since the steady state data based signals are slowly varying, it can be argued that corresponding methods fail to detect the high bandwidth content (small time scale) profiles in the sample in similar situations that may arise during scanning.

Observe that the peaks are easily discernible in the innovation sequence [see Fig. 3(b)]. When the cantilever is not interacting with the sample (until  $\approx 950$   $\mu\text{s}$ ) the innovation sequence has zero mean and is white. As soon as it encounters the first peak in the sample profile ( $\approx 950$   $\mu\text{s}$ ) the innovation sequence becomes nonwhite and dynamic profile is detected. Between the first and the second peaks in the sample profile, the innovation sequence recovers the zero mean and white nature until the second peak appears ( $\approx 1050$   $\mu\text{s}$ ). Overlapping dynamic profiles may appear in the innovation sequence ( $\approx 1050$   $\mu\text{s}$ ) due to multiple hits with the sample in consecutive cycles. The likelihood ratio [see Fig. 3(c)] increases significantly when the dynamic profile is present in the innovation sequence. The peaks are detected within two cycles. The overlapping dynamic profiles are detected as a single event (second peak) as shown by the detection signal [see Fig. 3(e)]. Note that the cantilever has not reached steady state and is in transient during the entire experiment.

The dynamic profile [see Fig. 3(a)] persists for approximately 25  $\mu\text{s}$  ( $\approx 2/f_0$  s) which is captured within a data window of size  $M=128$  with a 5 MHz sampling. The dy-

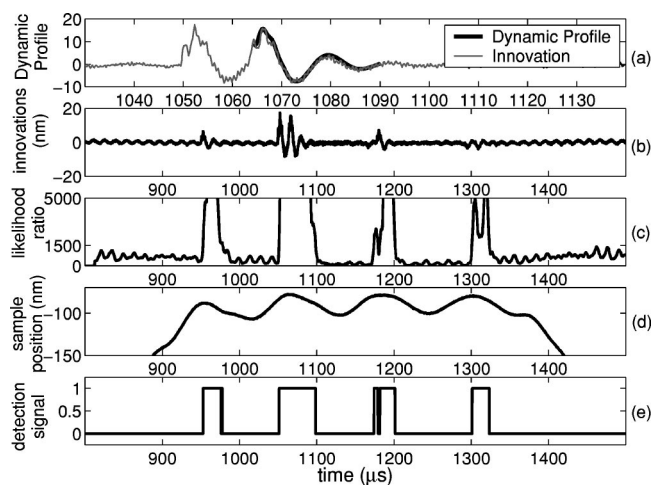


FIG. 3. (a) The dynamic profile buried in innovation sequence, (b) the innovation sequence, (c) likelihood ratio, (d) sample profile, and (e) the detection signal are shown when the cantilever is probing the sample during its transient state. The four peaks are detected by the appearance of dynamic profile in the innovation sequence and it being captured by likelihood ratio as shown by the detection signal.

amic profile is detected in 23.94  $\mu\text{s}$  ( $\approx 2/f_0$  s) of its inception (with threshold  $\epsilon=1681.3$  corresponding to a false alarm rate of  $P_F=0.1\%$  and detection probability  $P_D=90\%$  for a minimum step size to detect  $\nu=0.25$  nm). To ensure at least one hit with cantilever the sample has to be present for more than 1 cycle ( $1/f_0$  s) of the cantilever oscillation. A good estimate of the bandwidth is  $f_0/4$  Hz = 17.5 kHz. The experiment demonstrates a detection bandwidth  $\approx 10$  kHz. This is considerably large as compared to the cantilever's natural bandwidth as determined by  $f_0/Q \approx 390$  Hz. Note that high quality factor of the cantilever does not limit the bandwidth in the proposed scheme. It is evident from the innovation sequence and the likelihood ratio that the cantilever interactions with the peaks in the sample profile are not uniform. However, by feeding back the demodulated amplitude signal to the sample positioner and the cantilever this issue can be effectively addressed.

This research is supported by NSF Grant No. NSF ECS-0330224 to M.V.S.

- <sup>1</sup>G. Binnig, C. Quate, and C. Gerber, *Phys. Rev. Lett.* **56**, 930 (1986).
- <sup>2</sup>R. Wisendanger, *Scanning Probe Microscopy and Spectroscopy* (Cambridge University Press, Cambridge, 1994).
- <sup>3</sup>T. Sulchek, R. Hseih, J. D. Adams, G. G. Yaralioglu, S. C. Minne, C. F. Quate, J. P. Cleveland, and D. M. Adderton, *Appl. Phys. Lett.* **76**, 1473 (2000).
- <sup>4</sup>R. D. Jäggi, A. Franco-Obregón, P. Studerus, and K. Ensslin, *Appl. Phys. Lett.* **79**, 135 (2001).
- <sup>5</sup>T. Rodríguez and R. García, *Appl. Phys. Lett.* **79**, 135 (2001).
- <sup>6</sup>M. V. Salapaka, H. S. Bergh, J. Lai, A. Majumdar, and E. McFarland, *J. Appl. Phys.* **81**, 2480 (1997).
- <sup>7</sup>C.-T. Chen, *Linear System Theory and Design* (Oxford University Press, New York, 1999).
- <sup>8</sup>A. H. S. Thomas Kailath and B. Hassibi, *Linear Estimation* (Prentice-Hall, Englewood Cliffs, NJ, 2000).
- <sup>9</sup>M. V. Salapaka, D. Chen, and J. P. Cleveland, *Phys. Rev. B* **61**, 1106 (2000).
- <sup>10</sup>A. S. Willsky and H. L. Jones, *IEEE Trans. Autom. Control* **21**, 108 (1976).
- <sup>11</sup>S. M. Kay, *Fundamentals of Statistical Signal Processing, Detection Theory* (Prentice-Hall, Englewood Cliffs, NJ, 1993), Vol. II.